



# Description, Modelling and Simulation of a Benchmark System for Converter Dominated Grids (Part I)

98% - RES Benchmark on Basis of fast  
Voltage Source controlled Converters (EMT & RMS)

Prof. Dr.-Ing. habil István Erlich <sup>(†)</sup>

M.Sc. Abdul Wahab Korai

[abdul.korai@uni-due.de](mailto:abdul.korai@uni-due.de)



Institute of Electrical Power System

University Duisburg-Essen

04.06.2018



## Contents

List of Acronyms.....	4
1 Introduction.....	5
2 System overview.....	7
3 Models and data.....	8
3.1 Network data.....	8
3.2 Load flow data.....	8
3.3 Synchronous generator data.....	9
3.4 Exciter and governor data.....	10
3.5 Load data.....	10
3.6 Full-scale converter -based WT dynamic model.....	10
3.6.1 Converter and DC circuit for the EMT and RMS model.....	10
3.6.2 Control system.....	11
3.6.3 Protection logic.....	12
3.6.4 WT control for the EMT and RMS model.....	12
3.6.5 Comparison of the EMT and RMS models of the benchmark test system.....	18
3.6.6 Implementation of the control in PowerFactory.....	19
4 References.....	20



## List of Figures

Figure 1: Benchmark test system .....	7
Figure 2: Full-scale converter based WT system configuration .....	10
Figure 3: Two level converter topology .....	11
Figure 4: DC Circuit block diagram.....	11
Figure 5: Reactive power control .....	13
Figure 6: Active power control .....	14
Figure 7: Phase locked loop .....	16
Figure 8: Converter current limitation method .....	17
Figure 9: Converter modulation index limitation.....	18

## List of Tables

Table 1: Overhead transmission line parameters .....	8
Table 2 : Transformer parameters .....	8
Table 3: Operating point of synchronous generator and wind park buses .....	8
Table 4 : Operating point of the network buses .....	9
Table 5 : Synchronous generator dynamic data .....	9
Table 6 : Protection circuits, trigger conditions and timings .....	12
Table 7 :Var –Voltage control parameters .....	13
Table 8 : Active power control parameters .....	14
Table 9 : PLL parameters .....	16
Table 10 : Current limitation parameters .....	17
Table 11 : Modulation index limitation parameters .....	18
Table 12: Comparison of RMS and EMT models.....	18



## List of Acronyms

---

RMS	Root Mean Square
EMT	Electro Magnetic Transient
PWM	Pulse Width Modulation
PLL	Phase Locked Loop
WT	Wind Turbine
DC	Direct Current
AC	Alternating Current
VSC	Voltage Source Converter
LSC	Line Side Converter
DSL	DIgSILENT Simulation Language
MSC	Machine Side Converter
MVA	Mega Volt Ampere
p.u.	Per Unit
VDAPR	Voltage Dependent Active Power Reduction
AVR	Automatic Voltage Regulator
WP	Wind Park
OWP	Offshore Wind Park
RES	Renewable Energy Source



## 1 Introduction

The increasing penetration of the converter-based generation in the electrical power system, have given rise to many challenges to power system. Two of the most important challenges are the voltage and frequency control. As is well known, most of renewable-based generation units feed power into the network via converter interfaces. This means that the inertia, to the extent it is available, is not effective as viewed from the AC network side. The currently applicable grid codes, on the other hand, were designed primarily to ensure that renewables are operated in such a way that they do not interfere with the safe and secure operation of the conventional plants.

In the meantime, the role of renewables is changing rapidly to an extent that they are moving towards becoming the dominant factor in the network. This is why there is a growing demand for so-called grid forming behavior on the part of renewable generation units. This means, above all, that renewables must take responsibility for voltage-Var and frequency regulation. It should be noted that these tasks have to be performed in the face of continuously decreasing grid inertia (resulting from reduced number of conventional units) which leads to a much faster dynamic behavior and therefore requires faster controller response times. Grid forming requirement, in principle, is premised on the assumption that renewables should take responsibilities commensurate with their share in the overall installed capacity even in extreme situations, for example, in situations where they are required to manage grid restoration.

The currently applicable network connection rules clearly are not up to the emerging new challenges. Work on further revision is therefore already under way. However, it is to be expected that the renewable technologies currently deployed will shape the dynamic grid behavior for the next 5-10 years.

One of the major concerns is the current injection control based on PI characteristic of a converter current control which does not necessarily lead to problems as long as the converter is feeding into a strong network capable of absorbing the injected current. With the projected future scenarios ranging from 50% to 100% renewables, it is obvious that a new converter control scheme is required which adapts automatically to the current depending on the grid conditions by trying to fulfil the main objectives of voltage and frequency control [1].



An example of such specific phenomenon encountered during the practical operation of an offshore wind park connected to the grid via a VSC-HVDC link, namely an OWP being forced into an island operation mode due to converter blocking. Regardless of the origin of the blocking signal, however, the challenge is to ascertain that the ensuing transient process and the accompanying voltage surge do not cause excessive stress on the converter [2]. In this situation, the frequency of the islanded network is no longer controlled as the wind turbines currently are not equipped with such a control capability. Additionally, the voltage controllers in the common implementation perform voltage control indirectly by injecting reactive current but injecting reactive current and thus effective voltage control is not possible in islanded offshore grid if no considerable local load exists and the link to the onshore grid is severed. However, the control of the state of the art wind turbines presupposes that the current reference can be injected into the grid at any time. However, this is not the case in an island grid and becomes even difficult in converter dominated grids especially in those cases, where the share of the converter based generation is very high [1].

For this purpose, a grid forming converter control of the wind turbine has been proposed [3] and based on this control, a benchmark test system has been developed for the assessment of the effect of the converter dominated grid on the power system stability.

## 2 System overview

The proposed benchmark test system is fictitious but similar to the typical European transmission network. All connections represent 380 kV overhead lines with typical parameters and each 100 km long. The power in-feed to the network from two wind parks takes place at two locations marked "WP". The WP in this test system is represented as aggregated full-scale based WT model as depicted in the Figure 1. In order to take account of the multiple step-up transformation from the wind turbine to the high voltage bus, an equivalent transformer reactance of 30% is used. For this benchmark test system, the share of wind is 98 % of the total power generation and the conventional generation is only 2% [1]. Figure 1 shows the benchmark test system, which has been modelled both for EMT and RMS type of modes.

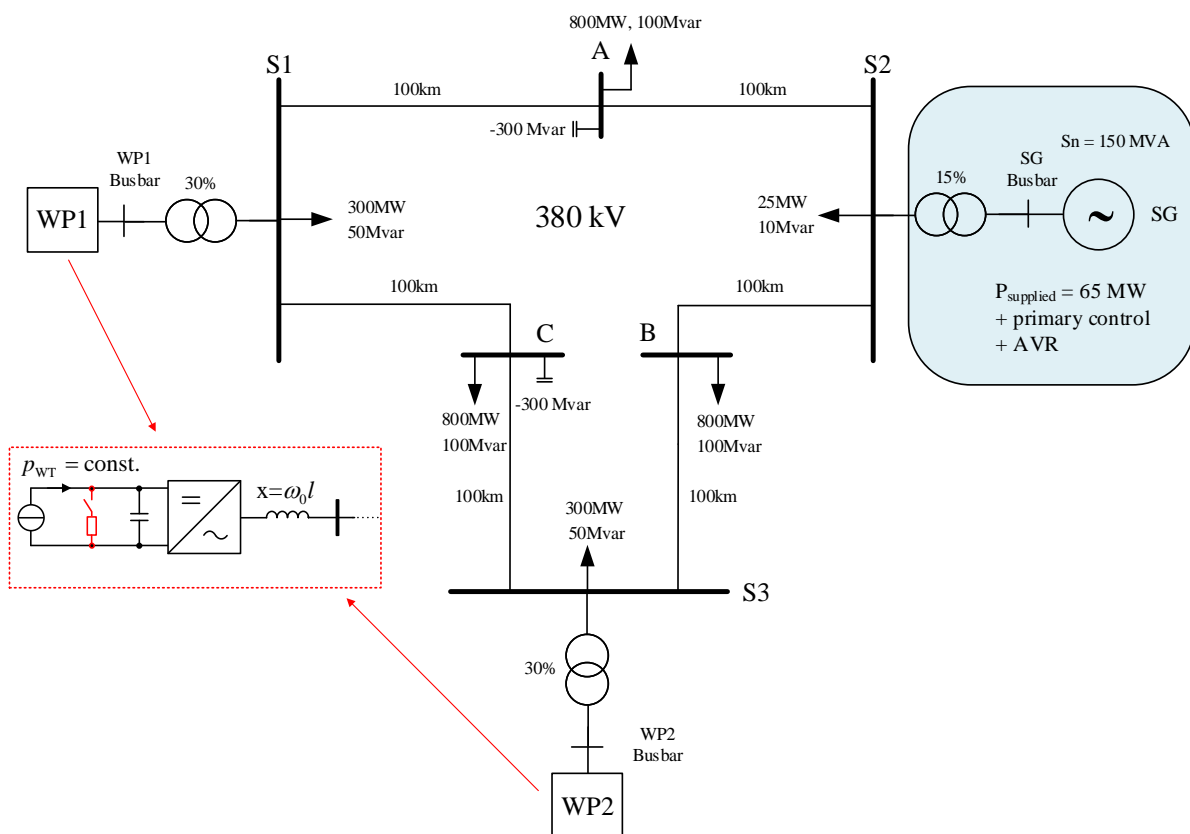


Figure 1: Benchmark test system

### 3 Models and data

The test system contains one synchronous generator, 2 full-scale converter based wind parks (aggregated) with 6 transmission buses, 3 step-up transformers, 2 shunt elements, 6 transmission lines and 6 loads.

#### 3.1 Network data

Table 1 shows the overhead transmission data. Whereas Table 2 shows the transformer parameters used in this test system.

**Table 1: Overhead transmission line parameters**

Name	$R$ ( $\Omega$ )/km	$X$ ( $\Omega$ )/km	Capacitance ( $\mu F$ )/km
380 kV transmission line	0.031	0.266	0.014

**Table 2 : Transformer parameters**

Transformer name	From bus	To bus	$r$ (p.u.)	$x$ (p.u.)	$S_{nom}$ (MVA)
SG transformer	SG busbar	S2	0.0023	0.15	150
Wind park 1 transformer	WP1 busbar	S1	0.0020	0.3	1580
Wind park 2 transformer	WP2 busbar	S3	0.0020	0.3	1580

#### 3.2 Load flow data

Table 3 shows the operating point data of the generator and wind park buses while in Table 4, the operating point data of the network buses is shown.

**Table 3: Operating point of synchronous generator and wind park buses**

Name	Busbar name	Nominal apparent power (MVA)	Generated active power (MW)	Generated reactive power (Mvar)	Voltage magnitude (p.u.)	Voltage angle (deg)
SG	SG busbar	150	65.1	30.2	1.03	0.0
Wind park 1	WP1 busbar	1580	1500	228.1	1.0	170.9



Wind park 2	WP2 busbar	1580	1500	296.3	1.0	171.3
-------------	------------	------	------	-------	-----	-------

**Table 4 : Operating point of the network buses**

Bus	Bus voltage (kV)	Consumed active power (MW)	Consumed reactive power (Mvar)	Generated active power (MW)	Generated reactive power (Mvar)	Voltage magnitude (p.u.)	Voltage angle (deg)
S1	380	0	0	0	0	1.03	154.3
S2	380	0	0	0	0	1.03	146.4
S3	380	0	0	0	0	1.01	154.5
A	380	0	0	0	0	1.04	146.2
B	380	0	0	0	0	1.01	146.3
C	380	0	0	0	0	1.03	150.2

### 3.3 Synchronous generator data

Synchronous generator dynamic data is given in the Table 5.

**Table 5 : Synchronous generator dynamic data**

Parameters	Generator type	Unit
	Round rotor	
$x_d$	1.97	p.u.
$x_q$	1.97	p.u.
$x_d'$	0.29	p.u.
$x_q'$	0.29	p.u.
$x_d''$	0.2	p.u.
$x_q''$	0.28	p.u.
$T_d'$	0.93	p.u.
$T_q'$	0.189	s
$T_d''$	0.12	s
$T_q''$	0.18	s
$H$	5	s

### 3.4 Exciter and governor data

Standard IEEE models (EMAC1T) and (IEEEG1) have been used for the voltage and speed control of the synchronous generator respectively [4]. The governor and AVR parameters have been adjusted to emulate the frequency response adequately for the high RES share. Additionally, a PSS can be activated to improve generator rotor oscillation damping.

### 3.5 Load data

The load models are governed by the following equation

$$P = P_0 \left( \frac{U}{U_0} \right)^\alpha \quad Q = Q_0 \left( \frac{U}{U_0} \right)^\beta \quad (1)$$

where  $\alpha = \beta = 2$

Which represents a constant impedance load [4].

### 3.6 Full-scale converter -based WT dynamic model

Figure 2 shows the model of the full-scale converter based wind turbine. The MSC and wind turbine generator part are simplified because for the grid dynamics, only line side converter is relevant [3]. However, the chopper and DC circuit has been included in the model of the WT so that the dynamics of the DC circuit can be observed and are well represented. It is assumed that the machine side converter injects a constant active power into the DC circuit.

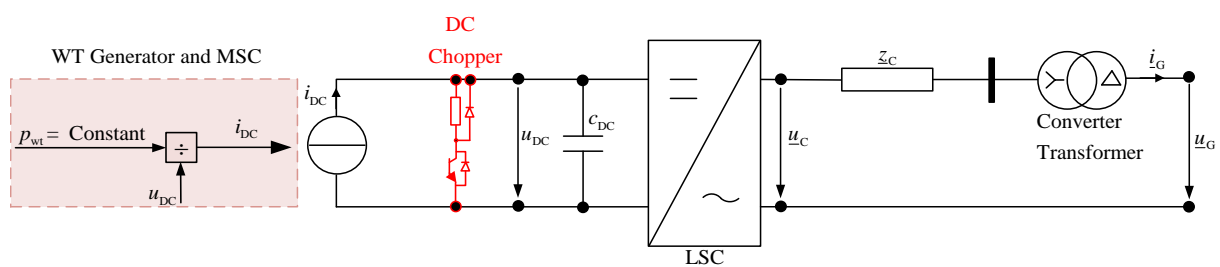
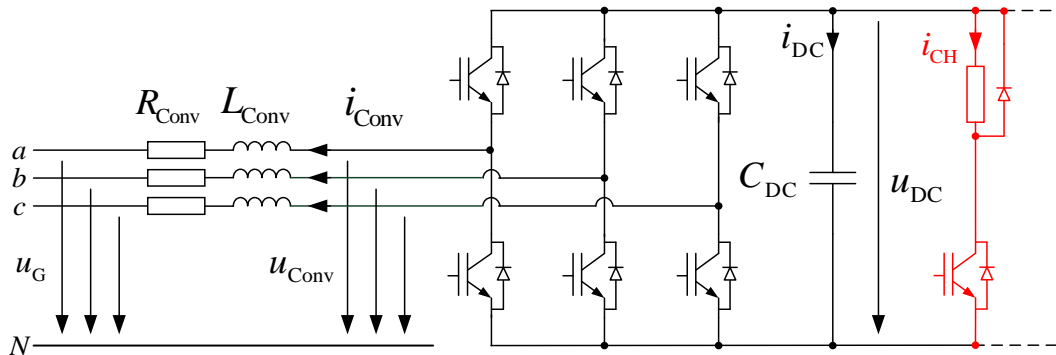


Figure 2: Full-scale converter based WT system configuration

#### 3.6.1 Converter and DC circuit for the EMT and RMS model

The converter model implemented exhibits two level architecture as shown in Figure 3, which is only applicable for the PWM mode [4].



**Figure 3: Two level converter topology**

It is however to be noted that the PWM model has not been used in this benchmark test system whereas the LSC in EMT and RMS is represented by controlled voltage source.

The connection and the power balance between the LSC and MSC of the WT is described by the block diagram shown in Figure 4. The converter losses are neglected.

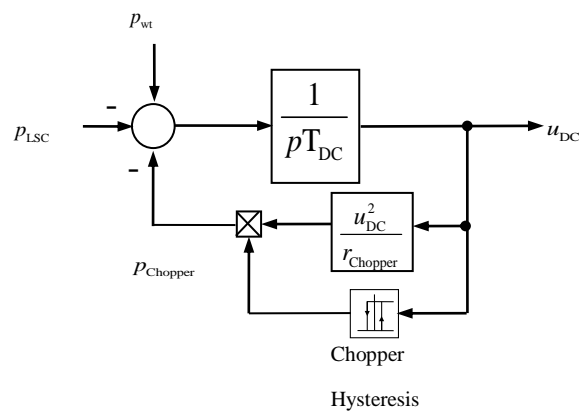


**Figure 4: DC Circuit block diagram**

### 3.6.2 Control system

The control system of the full-scale converter -based WT can mainly be divided into two parts:

- Protection logic
- WT control

In the following subsections, the main control schemes which are implemented in the actual model are described.

### 3.6.3 Protection logic

The protection logic represents the trigger conditions for the protection circuit, in this case, chopper circuit. The blocking of the converters has not been modelled but can be extended easily. The trigger conditions for the chopper circuit are given in Table 6.

**Table 6 : Protection circuits, trigger conditions and timings**

Protection circuit	Trigger condition & timing
Chopper	Activated, if $u_{DC} > u_{DC\_CHon}$  Deactivated, if $u_{DC} < u_{DC\_CHoff}$

### 3.6.4 WT control for the EMT and RMS model

The control of the LSC both in RMS and EMT modes remains the same and is described in detail below.

#### 3.6.4.1 Var- Voltage control channel

In the proposed solution for the var – voltage control channel, first the reactive power reference is set based on a droop characteristic. This serves as an input to a PI block that determines the voltage reference as depicted in Figure 5. The response time of this controller is set 5 – 30 s, large enough to avoid significant control action during network short-circuit and small enough to preclude unnecessary tap movement in on-load tap changing (OLTC) transformers. For events requiring quicker response the downstream direct voltage controller with a proportional characteristic is responsible. Please note that no dead-band is included. The damping term replaces the proportional component of the PI block in the standard implementation at the moment. It offers also additional possibilities in terms of selective damping, and for the converter required current limitation is achieved through output voltage limitation.

After the addition of the controlled terminal voltage (the feed-forward term), the d-component of the inverter voltage is determined. As can be seen in Figure 5, the reactive current no longer appears explicitly in this scheme, and as a result there is no risk of integrator windup in the event of an unforeseen islanding. The current adjusts itself according to the network conditions in response to a changing converter voltage. Therefore, the scheme is more like the conventional synchronous machine voltage control.

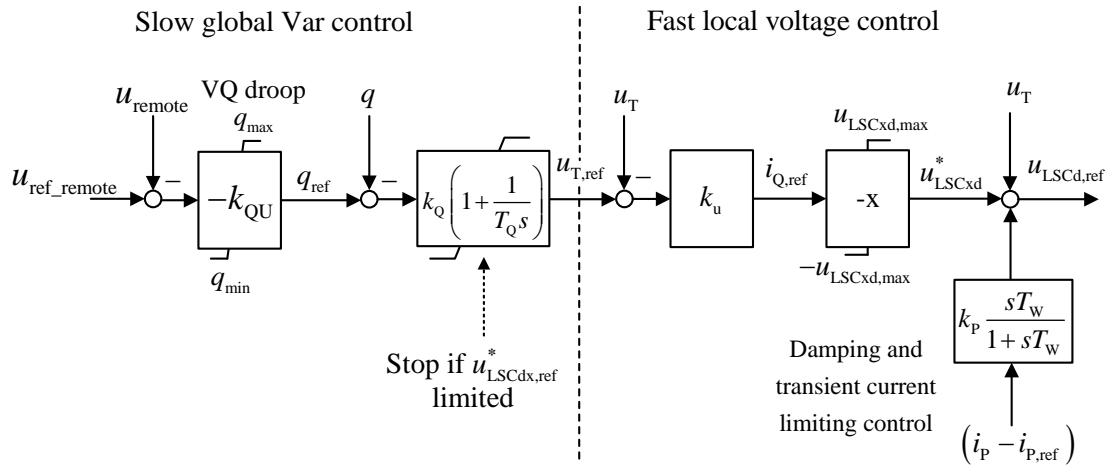


**Figure 5: Reactive power control**

The parameters of this control block are given in Table 7.

**Table 7 :Var –Voltage control parameters**

Parameter	Parameter description	Unit	Value
$k_{QU}$	Static gain for the global reactive power control	p.u.	6.6
$q_{max/min}$	Maximum/minimum reactive power in steady state	p.u.	0.31
$k_Q$	Global reactive power control proportional gain	p.u.	0.002
$T_Q$	Global reactive power control integral time constant	s	15
$k_u$	Local and continues voltage control proportional gain	p.u.	0.2
$x$	Converter reactance	p.u.	0.1
$k_p$	Washout filter proportional gain	p.u.	0.03
$T_w$	Washout filter time constant	s	0.01

### 3.6.4.2 Active power control channel

The output of the DC voltage controller is the active power injected into the network. The active power can be written as

$$p = u_T i_p = -u_T \frac{u_{Cq}}{x} \quad (2)$$

As can be seen in equation (2), the active power can be controlled using the q-component of the converter voltage. Please note that no integral current injection is used, and the actual active current adjusts itself in accordance with the power flow equations of the network. Figure 6 shows the control scheme for the active power control.

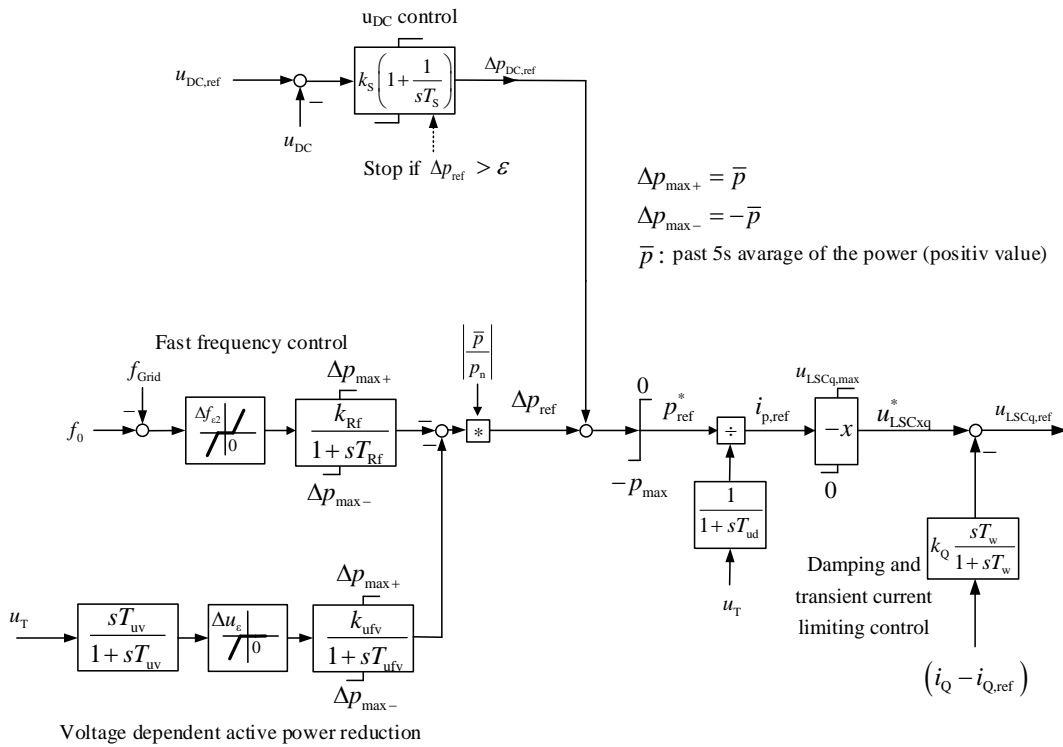


Figure 6: Active power control

The parameters of this control block are given in Table 8.

Table 8 : Active power control parameters

Parameter	Parameter description	Unit	Value
$k_s$	DC voltage control proportional gain	p.u.	4
$T_s$	DC voltage control integral time constant	p.u.	0.03
$k_{Rf}$	Proportional gain for the frequency control	p.u.	1
$T_{Rf}$	First order delay for the frequency control	s	0.2
$T_{uv}$	Washout time constant for the voltage dependent active power reduction (VDAPR)	s	60



$k_{ufv}$	Proportional gain for voltage dependent active power reduction	p.u.	2
$T_{ufv}$	First order delay for the voltage dependent active power reduction	s	0.005
X	Converter reactance	p.u.	0.1
$k_Q$	Washout filter proportional gain	p.u.	0.03
$T_w$	Washout filter time constant	s	0.01
$T_{ud}$	Voltage measurement delay	s	5
	Deadband for frequency control	Hz	0.2
	Deadband for the VDAPR	p.u.	0.1

The frequency control is activated when the frequency exceeds a preset threshold value, e.g. 50.2 or 49.8 Hz. The gain  $k_{rf}$  defines the frequency deviation at which the power reduction corresponds to the total power  $p_{ref}$  (e.g. 51.5 Hz). The time constant  $T_{rf}$  is small to tally with the fast response time of converters. One can also define in the delay block a limitation of rate of change. Also in Figure 6 can be seen the voltage dependent active power reduction, which is used as a way of feedforward and adjusts the power injection capability of the converter based on the terminal voltage of the converter. During a fault, the converter cannot inject power in the grid; hence, the VDAPR reduces the reference power set point of the converter immediately, thus improving the transient stability of the overall system [5].

The voltages  $u_{LSCxd}^*$  and  $u_{LSCxq}^*$  are limited to preclude the controller leading to the violation of maximum allowable current limit.

### 3.6.4.3 Phase locked loop

Figure 7 shows the PLL structure used for the wind turbine control.

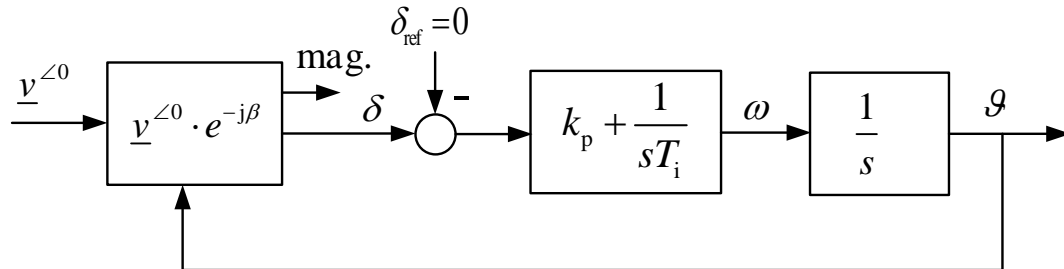


**Figure 7: Phase locked loop**

Table 9 shows the parameters of the PLL used.

**Table 9 : PLL parameters**

Parameter	Parameter description	Unit	Value
$k_p$	Proportional gain of PI controller of the PLL	p.u./s	100
$T_i$	Integral time constant of PI controller of the PLL	s	0.005

### 3.6.4.4 Current limitation

Figure 8 shows the current limitation logic of the converter control. When the actual converter current exceeds the maximum current of the converter, a new maximum current value is calculated using the equation shown in Figure 8. The new calculated maximum current value is used in the limiter block along with the angle of the grid impedance seen by the converter. The reference current i.e. limits of the d- and q- converter control voltages are limited based on the impedance of the grid and new calculated maximum current value. This means, that the converter adjusts the reference currents based on the impedance seen by it and thus it provides the best possible voltage support [5]. This idea is again depicted with the help of the phasor and circle diagram in Figure 8.

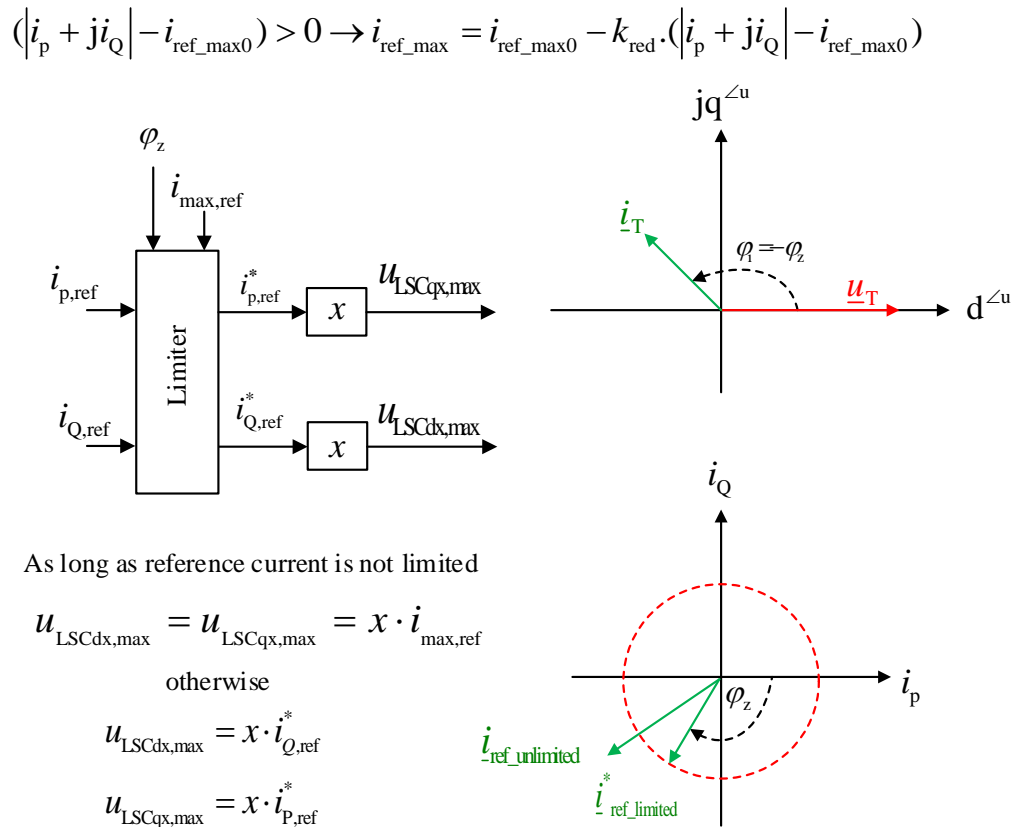


**Figure 8: Converter current limitation method**

Table 10 shows the parameters of the current limitation block

**Table 10 : Current limitation parameters**

Parameter	Parameter description	Unit	Value
$k_{\text{red}}$	Gain for the current limitation	p.u.	1.2

### 3.6.4.5 Modulation index limitation

Figure 9 shows the modulation limitation of the converter. The converter voltage is limited to 1 p.u.

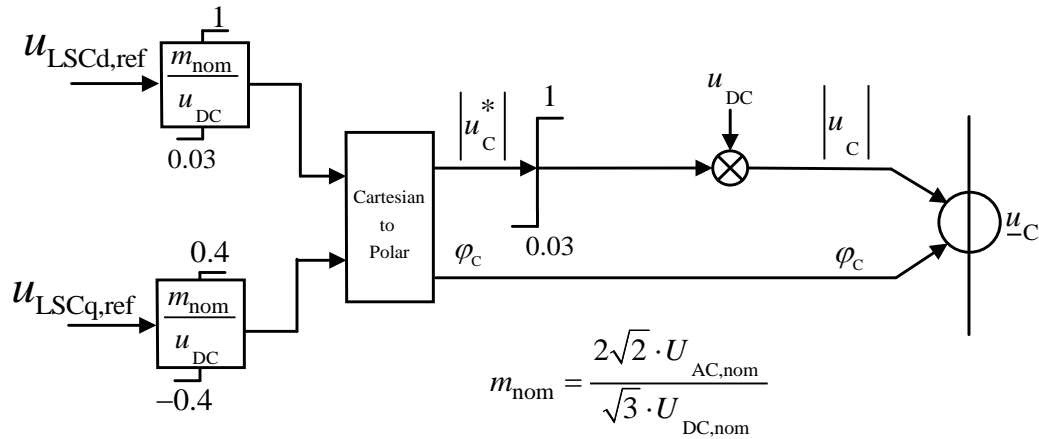


**Figure 9: Converter modulation index limitation**

Table 11 shows the parameters of the modulation limitation block

**Table 11 : Modulation index limitation parameters**

Parameter	Parameter description	Unit	Value
$U_{\text{AC,nom}}$	Nominal AC voltage of the Converter	V	690
$U_{\text{DC,nom}}$	Nominal DC voltage of the Converter	V	1276

### 3.6.5 Comparison of the EMT and RMS models of the benchmark test system

The benchmark test system has been created for both RMS and EMT type of modes. Table 12 shows the comparison between EMT and RMS models.

**Table 12: Comparison of RMS and EMT models**

Model	EMT	RMS
Grid	Differential equations	Algebraic equations
Converter	Controlled voltage source	Controlled voltage source
Separated Pos. and Neg. Sequence Control	No, only full space vector considered	No, only positive sequence is considered
Saturation of transformers and inductors	Can be activated/deactivated	Not represented
Common Mode Signal	No, but can be implemented	No but can be represented
Limitation of modulation index	Limited to 1	Limited to 1
Converter blocking	Possible but converter control is not adapted	Possible but converter control is not adapted



<b>Model</b>	<b>EMT</b>	<b>RMS</b>
DC circuit and Chopper	Represented	Represented
Measurement filters	No	No
PLL	Represented	Represented
Voltage control (voltage support)	Direct proportional control without deadband	Direct proportional control without deadband
Generation of harmonics	No generation of the harmonics through converters	50 Hz fundamental models
Integration step size	0.01 – 8 ms	5 – 200 ms
Possible disturbances	Any balanced and unbalanced grid faults but converter controls only the full space vector	Only balanced faults (Positive Sequence)
	Load connection	Load connection
	Load disconnection	Load disconnection

### 3.6.6 Implementation of the control in PowerFactory

Both EMT and RMS models have been modelled in DIgSILENT Power Factory version 2018 SP1. The implementation of the model in Powerfactory, the comparison of EMT and RMS models as well as different study cases are described in separate document [6].



## 4 References

- [1]. I. Erlich, A. Korai and F. Shewarega, "Control challenges in power systems dominated by converter interfaced generation and transmission technologies," *2017 IEEE Power & Energy Society General Meeting*, Chicago.
- [2]. I. Erlich *et al.*, "Overvoltage phenomena in offshore wind farms following blocking of the HVDC converter," *2016 IEEE Power and Energy Society General Meeting (PESGM)*, Boston, MA, 2016, pp. 1-5.
- [3]. I. Erlich, A. Korai *et al.*, "New Control of Wind Turbines Ensuring Stable and Secure Operation Following Islanding of Wind Farms," in *IEEE Transactions on Energy Conversion*, vol. 32, no. 3, pp. 1263-1271, Sept. 2017.
- [4]. DIgSILENT PowerFactory 2018 user manual.
- [5]. A. Korai, "Enhanced Control of the Wind Turbines and HVDC Systems for the Improvement of the Power System Stability", PhD. dissertation, University of Duisburg-Essen, 2018.
- [6]. DIgSILENT, "Description, Modelling and Simulation of a Benchmark System for Converter Dominated Grids (Part II)", June 2018